Numerical modelling for effect of water curtain in mitigating toxic gas release

Dong Seok Min [1], Shinhee Choi [1], Eui-young Oh, Jechan Lee, Chang-Gu Lee, Kwon-young Choi [**], Seungho Jung [*]

Department of Environmental and Safety Engineering, Ajou University, Suwon, Republic of Korea

ABSTRACT

Hydrogen fluoride and ammonia are widely used in chemical industries. Both substances are hazardous and frequently a source of leakage accidents. Since a hydrogen fluoride release accident occurred in Gumi, S. Korea (2012), the Korea Occupational Safety and Health Agency (KOSHA) has emphasized that special attention and management are needed with respect to toxic substances. For post-release mitigation, a water curtain is known as one of the most effective and economical systems. In this study, a computational fluid dynamics (CFD) program was used to identify the effect of using a water curtain as a mitigation system for toxic substances that leak out from industrial facilities. Simulations were conducted to analyze how effectively a water curtain could mitigate the dispersion of toxic substances. To verify the simulation's accuracy, the INERIS Ammonia dispersion experiment and Goldfish experiment were simulated and compared. Various water curtains were applied to the simulated field experiment to confirm the mitigation factors with toxic substances. The results show that the simulations and experiments are consistent and that the dispersion of toxic substances can be mitigated by water curtains in certain circumstances.

1. Introduction

As the chemical industry has developed, the use of toxic substances has substantially increased and leakage accidents have occurred more frequently. Among various hazardous substances, hydrogen fluoride (HF) and ammonia (NH_3) are representative materials for the study since both are hazardous and widely used in the chemical industry. HF is widely used in electronics manufacturing as a polisher and disinfectant and NH_3 is used in the semiconductor industry and various chemical processes. The representative cases in Korea include a HF leak accident occurred in Gumi in 2012 and an ammonia leak accident occurred in Namyangju in 2014. These accidents increased the public's awareness of the dangers of chemical accidents in Korea. In particular, since the Gumi HF release accident, the Korea Occupational Safety and Health Agency (KOSHA) has emphasized that special attention and management are required when handling toxic substances, and systematic changes have been implemented in laws and regulations (Bae and Chung, 2017; Lee et al., 2016).

To mitigate the impact of the accidental release of toxic chemicals, facilities are equipped with various systems such as dikes, secondary barriers, steam curtains, and water curtains. Among these, water spray systems are known to effectively decrease the gas concentrations and thus prevent the movement of a vapor cloud into the atmosphere after accidental toxic gas releases. To verify the effectiveness of a water spray system, several studies have been undertaken with various field tests and Computational Fluid Dynamics (CFD). Dandrieux et al. verified the mitigation effect when using peacock tail-type water curtains for a 0.25 kg/s release rate of ammonia gas (Dandrieux et al., 2001). Bouet et al. performed 15 field tests with physical barriers and water curtains for ammonia (Bouet et al., 2005). Kim et al. experimented on LNG dispersions with full cone-type water curtains and compared the concentrations near the release source with CFD dispersion simulations (Kim et al., 2012). Cheng et al. also did field tests for ammonia to compare CFD simulation results with the experiments (Cheng et al., 2014).

However, in these previous studies, the effectiveness with which gas dispersions were mitigated was significantly different for the peacock

---

tail-type water curtain. Dandrieux et al. showed very high mitigation efficiency in his experiment but there was almost no effect in Bouet et al. this is mostly because:

1. Toxic gases were pushed through the water curtain area due to the high jet momentum.
2. The water curtain shape was changed by metrological conditions.

This study explores how effectively a water curtain could mitigate the dispersion of toxic substances using ANSYS Fluent 18.0. We analyzed how the previous two studies have to be judged (Chung, 2002). In addition, simulations were conducted to determine the efficiency of water curtains for accidental ammonia and hydrogen fluoride releases under the same conditions. The purpose of this study is to help establish protection systems for the process of using toxic materials by determining the efficiency of a water curtain for substances and circumstances. To verify the simulation's accuracy, a Goldfish experiment and an INERIS Ammonia dispersion experiment were simulated and compared. After validation with field experiments, the meteorological conditions were fixed to avoid the concentration change in atmospheric condition. The concentration was compared between the presence and absence of a water curtain. Various water curtains were applied to the simulated field experiment to confirm the mitigation factors of toxic substances. The results show that the simulations and experiments were consistent and that the dispersion of toxic substances could be mitigated by water curtains (Blewitt et al., 1987; Goldwire et al., 1985).

2. Numerical simulation

ANSYS Fluent 18.0 is a program based on Navier–Stokes equations and is capable of carrying out the physical modeling of fluid flow. In this study, we sought to solve the relations between gas and water droplets, so we used the Eulerian–Lagrangian method. We defined the problem as a steady state and solved it using the Semi-Implicit Method for Pressure-Linked Equation method solver (SIMPLE).

2.1. Gas flow modeling

The governing equations are mass conservation, momentum conservation, and energy conservation (Versteeg and Malalasekera, 2007). The equation for mass conservation where ρ is the fluid density can be written as follows:

$$\frac{\partial \rho}{\partial t} + \nabla \cdot (\rho \mathbf{u}) = 0 \tag{1}$$

The equations for momentum conservation can be written as:

$$\frac{\partial (\rho u)}{\partial t} + \nabla \cdot (\rho u \mathbf{u}) = -\frac{\partial p}{\partial x} + \nabla \cdot (\mu \nabla u) + S_{Mx} \tag{2}$$

$$\frac{\partial (\rho v)}{\partial t} + \nabla \cdot (\rho v \mathbf{u}) = -\frac{\partial p}{\partial y} + \nabla \cdot (\mu \nabla v) + S_{My} \tag{3}$$

$$\frac{\partial (\rho w)}{\partial t} + \nabla \cdot (\rho w \mathbf{u}) = -\frac{\partial p}{\partial z} + \nabla \cdot (\mu \nabla w) + S_{Mz} \tag{4}$$

The above equations are for the conservation of momentum for the x-, y-, and z-axes. μ is the viscosity term and S_{Mx}, S_{My}, S_{Mz} are the terms for volumetric influences. The equation for energy conservation is as follows:

$$\frac{\partial (\rho i)}{\partial t} + \nabla \cdot (\rho i \mathbf{u}) = -p \nabla \cdot \mathbf{u} + \nabla \cdot (k \nabla T) + \Phi + S_i \tag{5}$$

2.2. Atmospheric boundary condition

For the atmospheric boundary condition, the wind power law relationship between the wind speeds at one height and those at another are written in (6–9), which depend upon the atmospheric stability (Blocken et al., 2007).

$$U(z) = U(z_1) \times \left(\frac{z}{z_1}\right)^p \tag{6}$$

$$k(z) = \frac{(U^*)^2}{\sqrt{C_\mu}} \tag{7}$$

$$\varepsilon(z) = \frac{(U^*)^3}{\kappa z_1} \tag{8}$$

$$U^* = \left(\frac{\kappa(U(z_1))}{\ln\left(\frac{z_1}{z_o}\right)}\right) \tag{9}$$

where U is the wind speed; U* is the sheared wind speed; κ is von Karman constant, the value of which is set at 0.4 for this study; C_μ is an empirical constant with a commonly accepted value of 0.03 for ABL flow (Zhang, 2009); z_1 is the wind speed at a reference height; z_o is the surface roughness factor; p is the value determined by air stability and surface roughness and the values, p = 0.1 for the C air stability class and p = 0.14 for the D air stability class, are used as EPA recommended (EPA, 2009).

In this simulation, the realizable k-ε was employed for the turbulence model. This model is the modified and improved version of the standard k-ε turbulence model to make better predictions for the spreading rate of both planar and round jets. The realizable turbulence model is based on separate transport equations for the turbulence kinetic energy (k) and its dissipation rate. The k-ε model equations are described as follows (Shih et al., 1995):

$$\frac{\partial}{\partial t}(\rho k) + \frac{\partial}{\partial x_j}(\rho k U_i) = \frac{\partial}{\partial x_j}\left[\left(\mu + \frac{\mu_t}{\sigma_k}\right)\frac{\partial k}{\partial x_j}\right] + G_k + G_b - \rho \varepsilon - Y_M + S_k \tag{10}$$

$$\frac{\partial}{\partial t}(\rho \varepsilon) + \frac{\partial}{\partial x_j}(\rho \varepsilon U_i) = \frac{\partial}{\partial x_j}\left[\left(\mu + \frac{\mu_t}{\sigma_\varepsilon}\right)\frac{\partial \varepsilon}{\partial x_j}\right] + \rho C_1 S \varepsilon - \rho C_2 \frac{\varepsilon^2}{k + \sqrt{v\varepsilon}}$$
$$+ C_{1\varepsilon}\frac{\varepsilon}{k}C_{3\varepsilon}G_b + S_\varepsilon \tag{11}$$

$$C_1 = \max\left[0.43, \frac{\eta}{\eta + 5}\right], \ \eta = S\frac{k}{\varepsilon}, S = \sqrt{2S_{ij}S_{ij}} \tag{12}$$

where G_k and G_b represent the generation of turbulence kinetic energy due to the mean velocity gradients and buoyancy, respectively; Y_M is the contribution of the fluctuating dilatation in the compressible turbulence to the overall dissipation rate; μ is the molecular viscosity; μ_t is the turbulence viscosity; $C_2, C_{1\varepsilon}, C_{3\varepsilon}$ are constants; σ_k and σ_ε are the turbulent Prandtl numbers for k and ε, respectively; S_k and S_ε are the increasing rates at the source.

2.3. Water curtain modeling

The discrete phase model (DPM) was used to analyze the relationship between a water curtain and toxic gas dispersions. DPM Eulerian-Lagrangian frameworks are an approach for the CFD simulation of multiphase systems including both continuous phase and discrete phase. Toxic gas (continuous phase) is solved by the Eulerian method, and water droplet (discrete phase) is solved by Lagrangian. The equations for these are as follows in (13–15) (Gosman and Ioannides, 1983):

$$\frac{du_p}{dt} = \frac{u - u_p}{\tau_r} + \frac{g(\rho_p - \rho)}{\rho_p} + F \tag{13}$$

$$\tau_r = \frac{\rho_p d_p^2}{18\mu}\frac{24}{C_d \text{Re}} \tag{14}$$

$$\mathrm{Re} \equiv \frac{\rho d_p |\boldsymbol{u_p} - \boldsymbol{u}|}{\mu} \tag{15}$$

where u is the fluid speed, u_p is the particle speed, μ is the fluid viscosity, ρ is the fluid density, ρ_p is the particle density, and d_p is the diameter of the particle.

The specification of water curtains was set based on INERIS tests performed in 2005. The peacock tail-type has 1200 L/min of water flow-rate at 8 barg and the water droplet temperature is assumed to be the atmospheric temperature. The diameter of water droplets is calculated based on Britter's equation (Britter et al., 2011).

$$d_{pm} \equiv We_C \frac{\sigma}{\rho_g u_{rel}^2} \tag{16}$$

where d_{pm} is the average droplet diameter; ρ_g is the density of the surrounding gas; u_{rel} is the relative speed between the water jet and the gas; σ is surface tension of the droplets; We_c is the Weber number, and the value 12.5 is used. Table 1 contains more details of water spray curtain.

2.4. Actual field test used in validation

We used ammonia large-scale atmospheric dispersion experiments by INERIS from 1996 to 1997 for comparison of an actual experiment and CFD simulation. Out of 15 total trials conducted in accordance with the size, height, direction of the leak and presence of protection devices, we have chosen Test #4 for the reference and Test #11 for the peacock tail-type water sprays. In Test #11, two water sprays were installed 60 m away from the source. Table 2 contains the information of each experiment. In both experiments, compressed liquefied NH_3 was discharged from the pipe at 1 m height from the ground and was vaporized and diffused. The concentrations of liquefied NH_3 were measured by sensors installed at 20 m, 50 m, 100 m, 200 m, 500 m, and 800 m.

For HF, the results of the Goldfish experiment conducted in 1986 in Frenchman, Nevada in the USA were compared with the simulation. In this experiment, which consists of three trials with different conditions as shown in Table 3, the compressed liquid HF was discharged through a pipe at a height of 1 m from the ground. The liquefied HF was vaporized and spread in the downwind direction in the form of steam clouds and the concentrations were measured by sensors installed at 300 m, 1000 m, and 3000 m from the leak source.

2.5. Simulation specification

For all comparisons, the atmospheric conditions were unified to minimize variables. In the field tests, the temperature and humidity were various for each test. Since the tendency of gas diffusion differs greatly according to temperature and humidity, the atmospheric condition was fixed at 25 °C and 50%. The wind speed and reference height were set at 3 m/s and 10 m and the applied atmospheric stability was D class.

Scenarios were set up to compare the mitigation effect of the water curtain on NH_3 and HF leaks as shown in Tables 4 and 5. 13 trials were simulated with water curtains and the results were then compared to the results of other trials without water curtains. We installed the water

Table 1
Simulation specification of a water curtain.

DPM Input Data	
Parameter	Input Data
Injection type	Surface (semicircular ring)
Nozzle size (mm)	Radius: 70, width: 10
Water flow rate (kg/s)	19.9013
Droplet Diameter (μm)	935
Initial Droplet Velocity (m/s)	12

Table 2
Information from the ammonia large-scale atmospheric dispersion experiment.

No.	Mass flow rate (kg/s)	Wind speed at 7 m (m/s)	Air stability	Temperature (°C)	Relative humidity (%)
4	4.2	3	D	12.5	82
11	3	5	C	24	24

Table 3
Information of Goldfish experiment.

No.	Mass flow rate (kg/s)	Wind speed at 2 m (m/s)	Air stability	Temperature (°C)	Relative humidity (%)
1	27.67	5.6	D	37.1	4.9
2	10.46	4.2	D	36.1	10.7
3	10.27	5.4	D	34.1	17.7

curtains similarly to the INERIS field test. In the field test, two water curtains were installed 6.25 m apart from the center line, but for this study, a water curtain was installed at the center line so that the toxic gas would contact the water curtain as much as possible. There were three different water curtain scenarios as follows:

1. Installed at 30 m and 60 m from the source simultaneously
2. Installed at 30 m from the source
3. Installed at 60 m from the source

Trials 1–3 were set based on INERIS NH_3 field test. To confirm the difference in the water curtain efficiency between the previous two field tests, we added Trial 4 based on Dandrieux et al. where the discharge rate and release height were lower. Then, for the other simulations, Trials 5–7, were conducted to determine the main factor of the difference between Trials 1–3 and Trial 4. Trials 5–7 were set to the same release height as Trials 1–3, but the discharge rate was set lower. For HF, in Trials 8–10 the release source and discharge rate were kept the same as the HF field test and the other conditions were set the same as the ammonia simulations. The discharge rate of Trials 11–13 were set to 0.5 kg/s (Cornwell et al., 1998).

The ANSYS Design Modeler 18.0 was employed to generate the geometry for atmospheric diffusion modeling. The size of the external flow region is width (W) × depth (D) × height (H) = 850 × 100 × 50 m³ in the NH_3 validation case and W × D × H = 3500 × 4000 × 1600 m³ in the HF validation case. W × D × H = 100 × 40 × 20 m³ in Trial 4 and W × D × H = 580 × 80 × 40 m³ in the other simulations. As shown in Fig. 1, the boundary conditions were set to velocity inlet on the air inlet, side, and top and outflow on the outlet. The ground is set to be the wall boundary condition and the mass flow inlet is applied to the horizontal leakage source.

3. Results

3.1. Comparison with field experiments

3.1.1. Comparison with ammonia field experiment

Table 6 shows the results of the field test and the simulation for ammonia leaks. From the comparison of the concentrations at six locations at 1 m height, the ratios between Test #4 (reference) and the

Table 4
Scenarios of various simulations with water curtains for NH_3.

Trial No.	1	2	3	4	5	6	7
Water curtain distance (m)	30	60	30&60	5	30	60	30&60
Release height (m)	1	1	1	0.15	1	1	1
Discharge rate (kg/s)	4.2	4.2	4.2	0.25	0.25	0.25	0.25

Table 5

Scenarios of various simulations with water curtains for HF.

Trial No.	8	9	10	11	12	13
Water curtain distance (m)	30	60	30&60	30	60	30&60
Release height (m)	1	1	1	1	1	1
Discharge rate (kg/s)	27.67	27.67	27.67	0.5	0.5	05
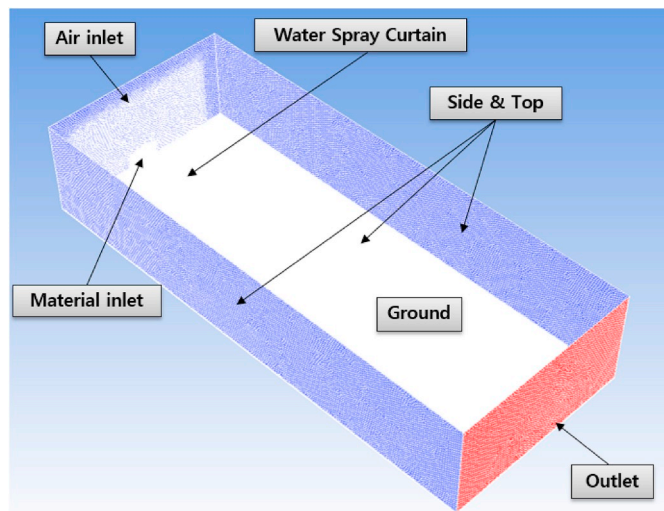
Fig. 1. 3D Geometry and boundary condition.

simulation were 0.71–1.17, which is reasonable. The ratios between Test #11 and the simulation were 0.68–2.00. The comparison showed good ratios up to 500 m. However, at 800 m, the ratio suddenly rose to 2.00. Therefore, the analysis domain was defined as 500 m.

3.1.2. Comparison with hydrogen fluoride field experiment

Table 7 shows the comparison of simulation data with Test #1 of the Goldfish (HF leak) field test. Simulation results ranging from 300 m to 3000 m showed similar trends to field tests, which were generally low in simulation results. The simulation results show that the ratios comparing the concentration of the experiment and simulation were 0.52–0.59. It is noted that a ratio within the range of 0.5–2 is normally considered to indicate good agreement with the experimental data (Witlox et al., 2014). Based on this, the model used for ammonia simulations was also applied to HF.

3.2. Mitigation efficiency of the water curtain

The mitigation effect of the water curtain was investigated after verifying the simulation of NH_3 and HF with actual experiments. The mitigation efficiency of the water curtain was calculated as shown in Equation (17):

$$\text{Efficiency} = 1 - \frac{C_{w.}}{C_{No\ W.}} \tag{17}$$

Table 7

Comparison with field test and simulation for HF.

Downwind Distance (m)	Test No. 1		
	Experiment (ppm)	Simulation (ppm)	Ratio (Sim/Exp.)
300	25473	13273	0.52
1000	3098	1842	0.59
3000	411	232	0.56

$C_{W.}$ is the concentration when using a water curtain, and $C_{No\ W.}$ is the concentration without a water curtain. Table 8 shows the efficiency of the water curtain according to the downwind distance at 1 m height.

Fig. 2 shows the mitigation effect in Trials 1–3 by comparing the results of these trials with the simulation result without a water curtain. The results indicate that the mitigation effect was not observed distinctly in Trials 1–3. This is the same trend as the result of the INERIS ammonia field test, which had the same discharge rate. Only slight efficiency differences for the water curtain were shown when installed at both 30 m and 60 m.

Fig. 3 shows the results of Trial 4. The efficiency of the water curtain is in the range 25–53%, with an average of 45% at 10–100 m. This is a much higher mitigation efficiency than those in Trials 1–3, which showed little efficiency. Trials 5–7 are the simulations carried out with the lower discharge rates under the same conditions as Trials 1–3. The results are shown in Figs. 4 and 5. The efficiency of water curtain is in the range 1–75%, and the average is approximately 30% for 100–500 m. The water curtains showed 59–75% efficiency at 100 m and 1–10% at 500 m, indicating that the effect decreases as the distance increases. Trial 5, where a water curtain was installed at 30 m, showed 6% better efficiency on average than Trial 6, where it was installed at 60 m. When water curtains were installed at both 30 m and 60 m, in Trial 7, the mitigation effect was increased by about 12% compared to when only one water curtain was installed.

As Trials 1–3 and Trial 4 are based on two previous field tests, we confirmed the difference in the mitigation effect of the water curtain between those two previous field tests. The results indicate that the water curtain was more efficient in Trial 4 which had the lower discharge rate and the lower release height. We conducted Trials 5–7 to determine the main factor of the difference, and the results showed good efficiency. Thus, the lower the discharge rate, the better the water curtain's efficiency. As the discharge rate increases, the amount of released toxic gas increases, so the momentum, which can be represented by the multiplication of mass and velocity, would increase. When the momentum is larger, the toxic gas can be less impacted by the water curtain. In addition, when the same amounts of toxic gas are dissipated by the water curtain, the ratio of lower discharge rate is definitely higher than that of higher discharge rate since the mitigation efficiency is expressed in ratio percentage (%). In other words, differences in the discharge rate or momentum could be an important factor affecting the mitigation effects.

Fig. 6 shows the mitigation effect in Trials 8–10 for HF. The water curtain's efficiency is about 17% on average in the range 100–500 m. The mitigation effect did not occur near the water curtain, but the

Table 6

Comparison between field tests and simulation for NH_3.

Downwind Distance (m)	Test No. 4			Test No. 11		
	Experiment (ppm)	Simulation (ppm)	Ratio (Sim/Exp.)	Experiment (ppm)	Simulation (ppm)	Ratio (Sim/Exp.)
20	65,000	46,000	0.71	65,000	44,000	0.68
50	27,000	27,000	1.00	27,000	25,000	0.93
100	16,000	17,000	1.06	15,000	13,000	0.87
200	10,000	8900	0.89	3500	3700	1.06
500	1200	1400	1.17	300	280	0.93
800	500	500	1.00	80	160	2.00

Table 8

The mitigation efficiency of a water curtain at 1 m height.

Downwind distance (m)	Trial 1	Trial 2	Trial 3	Trial 5	Trial 6	Trial 7	Trial 8	Trial 9	Trial 10	Trial 11	Trial 12	Trial 13
50	6%	–	6%	56%	–	57%	3%	–	3%	37%	–	37%
100	−2%	11%	14%	59%	59%	75%	3%	1%	6%	28%	43%	54%
200	−6%	−2%	0%	37%	33%	52%	11%	5%	11%	43%	46%	58%
300	−4%	−9%	−4%	26%	16%	34%	18%	12%	18%	32%	29%	40%
400	2%	−1%	9%	15%	6%	19%	28%	23%	28%	21%	17%	26%
500	4%	3%	11%	8%	1%	10%	31%	28%	32%	14%	10%	16%
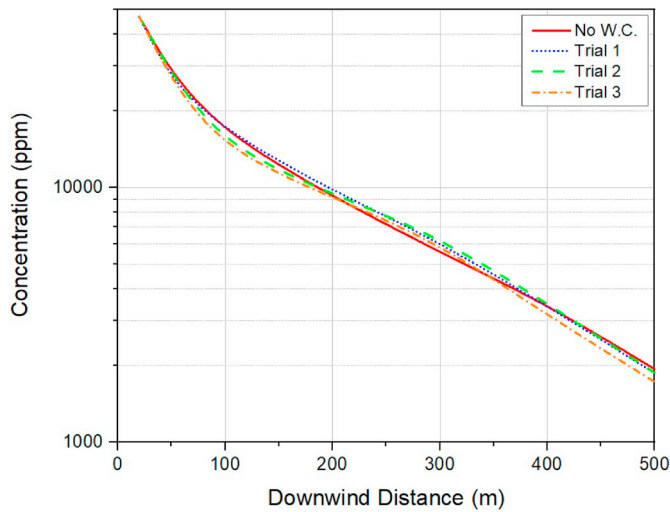
Fig. 2. Variation of NH_3 concentration according to the downwind distance by water curtain in Trials 1–3.
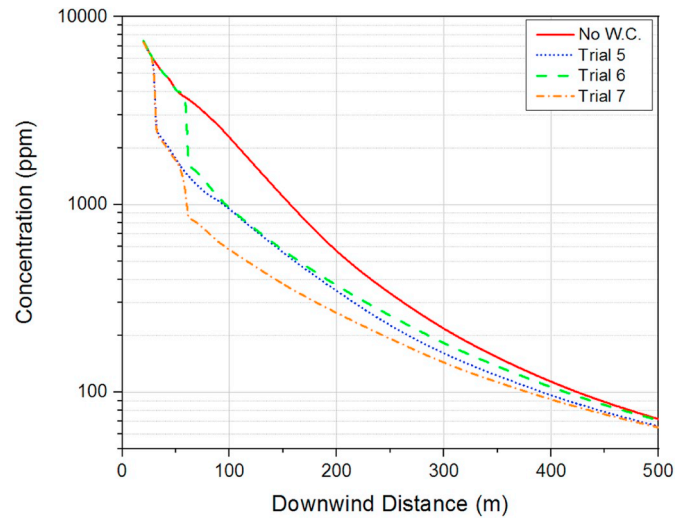
Fig. 4. Variation in the NH_3 concentration according to the downwind distance by water curtain for Trials 5–7.
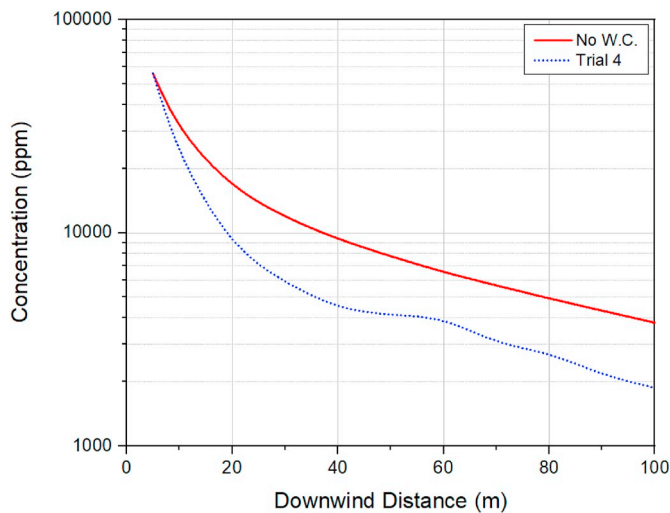
Fig. 3. Variation in the NH_3 concentration according to the downwind distance by water curtain for Trial 4.

efficiency was increased to about 30% at 500 m. This seems to indicate that the effect increases as the distance from the water curtain increases. Trial 8, where a water curtain was installed at 30 m, showed a 2–6% better efficiency on average than Trial 9, where it was installed at 60 m. When water curtains were installed at both 30 m and 60 m, in Trial 10, the mitigation effect was similar to that in Trial 8.

Trials 11–13 are simulations carried out with a lower discharge rate under the same conditions as those in Trials 8–10. The results are shown in Fig. 7. The efficiency of the water curtain is in the range 8–56%, and the average is about 30% at 100–500 m, showing maximum efficiency at

around 200 m. Trial 11, where a water curtain was installed at 30 m, generally showed better efficiency than Trial 12, where it was installed at 60 m. When water curtains were installed at both 30 m and 60 m, in Trial 13, the mitigation effect was increased by about 10% compared to when only one was installed.

Comparing the mitigation effects between Trials 8–10 and Trials 11–13, it was generally found that the smaller the discharge rate, the more efficient the water curtain, but the opposite result was found at 400 and 500 m. However, both NH_3 and HF tended to have decreased efficiency after the concentration became sufficiently low, so it is not always true that the water curtain is more efficient at an increased distance when the discharge rate is high.

The difference in the tendency of the water curtain mitigation effect according to the substances can be found. While the efficiency for NH_3 was good at points close to the water curtain, the efficiency for HF was maximized at points hundreds of meters further from the water curtain. The reason for this difference seems to be the difference between the substances' density at each boiling point. Since the release temperatures were set to the boiling points of the substances, NH_3 for −33.3 °C and HF for 19.5 °C, the density of NH_3 would have been dramatically reduced when encountering water at room temperature. As a result, NH_3 may have been more efficient than HF when it is near the water curtain.

4. Conclusion

In this study, the mitigation effects of the peacock tail-type water curtain for NH_3 and HF leaks were verified by simulations using computational fluid dynamics. We found the following results by analyzing the mitigation efficiency of the water curtain according to the distance from the source and the discharge rate.

First, the approach to the installation of water curtains varies depending on the type of substance and the area intended to reduce toxic concentration. Points where the water curtain shows maximum
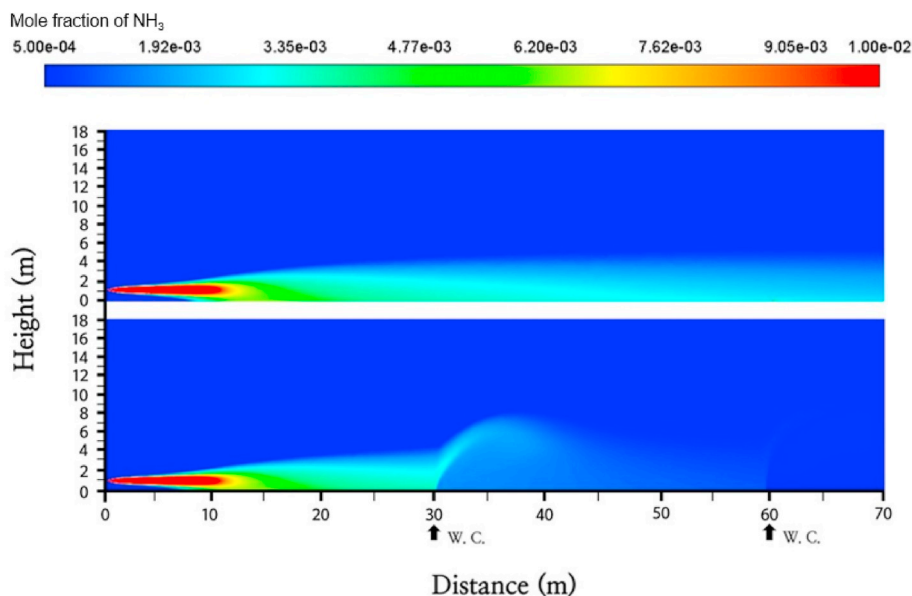
Fig. 5. Mitigation effect contour of the NH$_3$ concentration by water curtain in Trial 7.
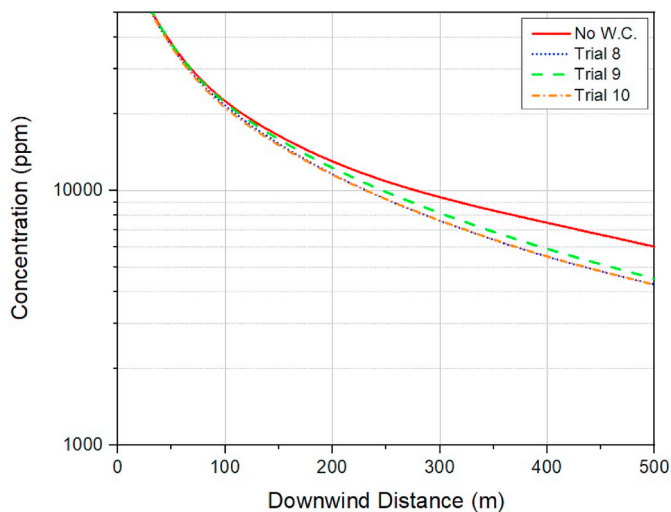
Fig. 6. Variation in the HF concentration according to the downwind distance by water curtain for Trials 8–10.

Fig. 7. Variation in the HF concentration according to the downwind distance by water curtain for 11-13.

efficiency differ depending on material type and the discharge rate. Therefore, choosing where to install the water curtain by considering the location of the protected target, the material properties, and the expected amount of leakage based on the storage volume is proposed.

Second, the water curtain installation distance shows a slight difference in terms of mitigation effects. The distance at which the water curtain is installed from the source affected the efficiency less than the type of substance and the discharge rate did. Therefore, it is speculated that the water curtain can be more effective by considering the type of substance and accident scenarios based on the discharge rate rather than optimizing the distance to the water curtain.

Last, multi-installation of a water curtain can improve the mitigation efficiency. A double water curtain showed higher efficiency than a single water curtain, which means that the protection target can be effectively protected by installing two or more water curtains and thereby increasing the efficiency. Moreover, for NH$_3$, multi-installation of a water curtain seems helpful to increase the overall efficiency and to prepare for severe accidents, which have a high discharge rate. This study can help understand how to install a water curtain in the optimal

place depending on the materials and circumstances to mitigate hazardous chemical accidents.

References

Bae, C.A., Chung, S.T., 2017. A study on awareness of risks and countermeasures for chemical accidents among residents near chemical plants. Cris. Emerg. Manag. 13, 123–134.

Blewitt, D.N., Yohn, J.F., Ermak, D.L., 1987. An evaluation of SLAB and DEGADIS heavy gas dispersion models using the HF spill test data. In: Proc. Int. Conf. On Vapor Cloud Modeling. AIChE, New York, pp. 56–80.

Blocken, B., Stathopoulos, T., Carmeliet, J., 2007. CFD simulation of the atmospheric boundary layer: wall function problems. Atmos. Environ. 41, 238–252.

Bouet, R., Duplantier, S., Salvi, O., 2005. Ammonia large scale atmospheric dispersion experiments in industrial configurations. J. Loss Prev. Process. Ind. 18, 512–519.

Britter, R., Weil, J., Leung, J., Hanna, S., 2011. Toxic industrial chemical (TIC) source emissions modeling for pressurized liquefied gases. Atmos. Environ. 45, 1–25.

Cheng, C., Tan, W., Liu, L., 2014. Numerical simulation of water curtain application for ammonia release dispersion. J. Loss Prev. Process. Ind. 30, 105–112.

Chung, T.J., 2002. Computational Fluid Dynamics. Cambridge University Press.

Cornwell, J.B., Johnson, D.W., Marx, J.D., 1998. The Use of Comparative Quantitative Risk Analysis in Evaluating Proposed Hydrogen Fluoride Mitigation Systems. Quest Consultants Inc.

Dandrieux, A., Dusserre, G., Ollivier, J., Fournet, H., 2001. Effectiveness of water curtains to protect firemen in case of an accidental release of ammonia: comparison of the effectiveness for two different release rates of ammonia. J. Loss Prev. Process. Ind. 14, 349–355.

EPA, 2009. RMP Guidance for Offsite Consequence Analysis.

Goldwire, H.C., McRae, T.G., Johnson, G.W., Hipple, D.L., Koopman, R.P., McClure, J.W., Morris, L.K., Cederwall, R.T., 1985. Desert Tortoise Series Data Report: 1983 Pressurized Ammonia Spills, UCID-20562. Lawrence Livermore National Laboratory, Livermore, CA.

Gosman, A.D., Ioannides, E., 1983. Aspects of computer simulation of liquid-fuelled combustors. J. Energy 7, 482–490.

Kim, B.K., Ng, D., Mentzer, R.A., Mannan, M.S., 2012. Modeling of water-spray application in the forced dispersion of LNG vapor cloud using a combined Eulerian−Lagrangian approach. Ind. Eng. Chem. Res. 51, 13803–13814.

Lee, K., Kwon, H. Myun, Cho, S., Kim, J., Moon, I., 2016. Improvements of safety management system in Korean chemical industry after a large chemical accident. J. Loss Prev. Process. Ind. 42, 6–13.

Shih, T.H., Liou, W.W., Shabbir, A., Yang, Z., Zhu, J., 1995. A new k-ε eddy viscosity model for high Reynolds number turbulent flows. Comput. Fluids 24, 227–238.

Versteeg, H.K., Malalasekera, W., 2007. An Introduction to Fluid Dynamics, second ed. Pearson Education Limited, England.

Witlox, H.W.M., Harper, M., Oke, A., Stene, J., 2014. Phast validation of discharge and atmospheric dispersion for pressurised carbon dioxide releases. J. Loss Prev. Process. Ind. 30, 243–255.

Zhang, X., 2009. CFD Simulation of Neutral ABL Flows. Energy.